ACS Sustainable Chemistry & Engineering

Research Article

pubs.acs.org/journal/ascecg

Vitamin B_2-Initiated Hydroxyl Radical Generation under Visible Light in the Presence of Dissolved Iron

Fang Xu,[†,‡] Xiang-Ning Song,[†] Guo-Ping Sheng,[†] Hong-Wei Luo,[†] Wen-Wei Li,[†] Ri-Sheng Yao,[‡] and Han-Qing Yu*[,†]

[†]CAS Key Laboratory of Urban Pollutant Conversion, Department of Chemistry, University of Science & Technology of China, Hefei 230026, China

[‡]School of Medical Engineering, Hefei University of Technology, Hefei 230009, China

Supporting Information

ABSTRACT: The generation of hydroxyl radical ($^{\bullet}OH$) under solar irradiation from natural photosensitizers is widely recognized to play a key role in the photochemical degradation of biorefractory organic pollutants. Solar-light-mediated $^{\bullet}OH$ production has been supposed as a green and sustainable strategy in water and wastewater treatment. In this study, an efficient visible-light-mediated $^{\bullet}OH$ generation method using the photosensitization of vitamin B_2 (VB_2) catalyzed by dissolved iron was proposed. $^{\bullet}OH$ generation was validated by electron paramagnetic resonance spectroscopy combined with spin trapping, and was further confirmed using the hydroxylation of nitrobenzene. VB_2 plays a dual role of in the process of $^{\bullet}OH$ generation. In the initial step, VB_2 works as an excellent photosensitizer. Upon absorption of a photon, VB_2 gives rise to its excited singlet state ($^1VB^*$) and, through intersystem crossing, to its excited triplet state ($^3VB^*$). In the subsequent step, VB_2 works as an effective electron mediator to mediate $O_2^{\bullet-}$ generation. However, $O_2^{\bullet-}$ is sensitive to proton and is converted to H_2O_2 quickly in water. Ultimately, the $^{\bullet}OH$ generation occurs through dissolved-iron catalyzed decomposition of H_2O_2. All ingredients involved in this process are nontoxic, environmentally benign, and easily available. Thus, this process might have potential environmental implications.

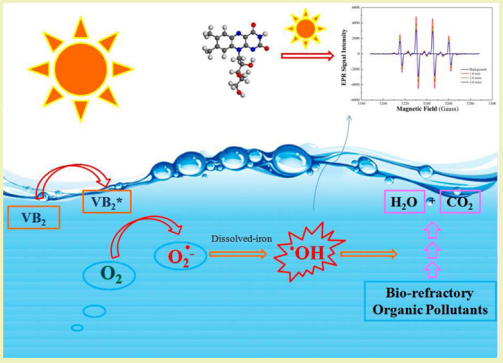

KEYWORDS: *Hydroxyl radical, Vitamin B_2, Reactive oxygen species, Photosensitizer, Electron mediator, Wastewater treatment*

INTRODUCTION

Human activity has dramatically increased inputs of biorefractory organic pollutants, such as pharmaceuticals, personal care products, and other synthetic organic compounds, etc., to the environment.[1−4] A multitude of characteristics of these substances, such as toxic, bacterial resistance, sterility, and feminization of aquatic organisms, bring about a host of problems.[5] The increasing use of these substances directly increases their concentration in treated and natural water and a novel, energy-efficient and sustainable method is highly desired,[6] as conventional wastewater treatment plants are not able to remove them entirely.[7,8] To address this issue, new effective methods for the treatment of biorefractory organic pollutants are always being pursued.

As a highly reactive oxidant, hydroxyl radicals ($^{\bullet}OH$) can unselectively react at near diffusion-controlled rates with most organic compounds, which has been proposed to play a key role in many oxidative processes,[9−11] e.g., in environmental treatment processes and as a reactive agent in phototherapies. It has been demonstrated that the use of advanced oxidation processes (AOPs) can break down a wide range of biorefractory organic pollutants due to the generation of $^{\bullet}OH$.[12,13] The reactions between $^{\bullet}OH$ and organic compounds in water are of great importance in engineered systems for environmental remediation. In surface water, a natural photosensitizer is ubiquitous and is a major source of photochemically generated $^{\bullet}OH$, which play an important role in the solar-light-mediated degradation of organic pollutants and can then provide a promising alternative for the treatment of biorefractory organic pollutants.[14−16] Humic substances have been commonly used as model compounds for a natural photosensitizer in environmental photochemistry.[17−25]

Vitamin B_2 (VB_2), also known as riboflavin, is an important water-soluble vitamin and widely present *in vivo* and natural environments.[26−28] VB_2 has been reported to function as an excellent photosensitizer to generate reactive oxygen species (ROS), such as singlet oxygen ($^1O_2$) and/or superoxide radical ($O_2^{\bullet-}$).[29−31] In biological systems, VB_2 can also serve as an effective electron mediator and its intracellular forms, such as flavin adenine dinucleotide and flavin mononucleotide, are involved in the generation of endogenous $^{\bullet}OH$.[26,27] Within mitochondria, $O_2^{\bullet-}$ has been presumed to be converted to

Received: April 1, 2015
Revised: June 11, 2015
Published: June 17, 2015

© 2015 American Chemical Society

DOI: 10.1021/acssuschemeng.5b00267
ACS Sustainable Chem. Eng. 2015, 3, 1756−1763

diffusible hydrogen peroxide (H_2O_2) and subsequently to the highly mutagenic and toxic $^{\bullet}OH$ in the presence of iron−sulfur (Fe−S) cluster.[32] VB_2-based cofactors play a central role in this intracellular process. Such a connection between VB_2 and iron thus inspires us to probe the possibility of synergy between VB_2 and dissolved iron for generating $^{\bullet}OH$ *in vitro*.

In this study, we report the $^{\bullet}OH$ generation through visible-light-mediated photosensitization of VB_2 catalyzed by dissolved iron. Such a process is investigated using electron paramagnetic resonance (EPR) spectroscopy combined with spin trapping. 2,2,6,6-Tetramethyl-4-piperidone (4-oxo-TEMP) is used to detect $^1O_2$,[33−35] whereas 5,5-dimethyl-1-pyrroline-*N*-oxide (DMPO) is utilized to measure $O_2^{\bullet-}$ and $^{\bullet}OH$.[35−37] To confirm further the VB_2-initiated $^{\bullet}OH$ generation, the hydroxylation reaction of nitrobenzene (NB) is employed to assess the reactivity of $^{\bullet}OH$.[40,41] With the experimental results, a possible mechanism is proposed to clarify the dual role of photosensitizer and electron mediator of VB_2 in such a visible-light-mediated $^{\bullet}OH$ generation process (Figure 1).

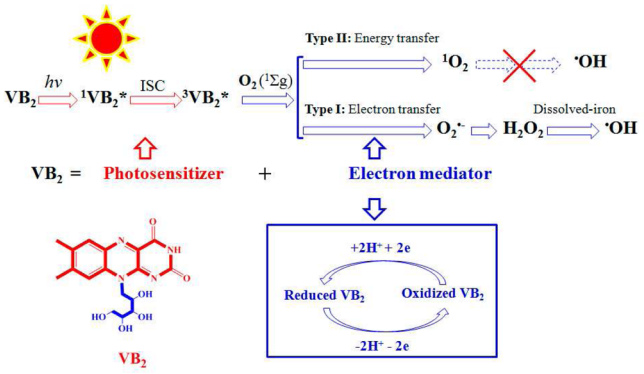

Figure 1. Schematic illustration of VB_2-initiated $^{\bullet}OH$ generation under visible irradiation in the presence of dissolved-ion (VB_2, vitamin B_2; ISC, intersystem crossing).

EXPERIMENTAL SECTION

Materials and Reagents. VB_2, 4-oxo-TEMP, DMPO and catalase were purchased from Sigma-Aldrich Co. (USA). DBACO, BQ and copper cyanide (CuCN) were purchased from Aladdin Chemical Reagent Co. (China). Ferrous sulfate heptahydrate ($FeSO_4{\cdot}7H_2O$), Ferric chloride ($FeCl_3$), sodium hydroxide (NaOH), hydrochloric acid (HCl), dimethyl sulfoxide (DMSO), HPLC-grade acetic acid and HPLC-grade ammonium acetate were purchased from Shanghai Chemical Reagent Co. (China) without further purification. HPLC-grade methanol was purchased from Merck Inc. (Germany). Ultrapure (MiniQ Inc., USA) water (resistivity of 18.2 MΩ·cm) was used in the experiments.

EPR Analysis. EPR spectra were obtained using a JES-FA200 EPR spectrometer (JEOL Co., Japan) with a 500 W Xe-arc lamp equipped with an UV-cutoff (>400 nm) as a visible-light source. A spectrometer with X-band microwave frequency of 9.072 GHz, microwave power of 2.02 mW, spectral window of 100 G and modulation amplitude of 4.00 G was used at ambient temperature of 20 °C.

$^1O_2$ was detected with the EPR method using 4-oxo-TEMP as a spin-trapping reagent (Reaction 1).[33−35] Solutions of VB_2 were prepared in ultrapure water. Under light irradiation, the incubation of VB_2 at 100 μM with the spin-trapping agent 4-oxo-TEMP of 100 mM resulted in the formation of the radical adducts. The generation of $^1O_2$ was detected as an EPR signal, because 4-oxo-TEMPO is formed by the reaction of $^1O_2$ with 4-oxo-TEMP.

DMPO was used as a spin-trapping agent for the detection of $O_2^{\bullet-}$ (Reaction 2).[35,36] $O_2^{\bullet-}$ is sensitive to the presence of proton and its

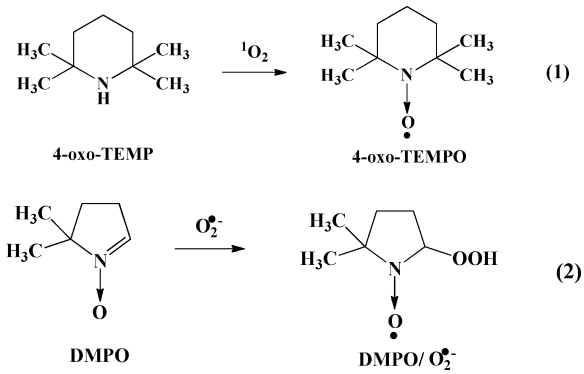

lifetime is very short in protic solvents.[38,39] Thus, it is difficult to detect $O_2^{\bullet-}$ in protic solvent and an aprotic solvent of dimethyl sulfoxide (DMSO) is used to facilitate the $O_2^{\bullet-}$ detection.[35,36] Solutions of VB_2 were prepared in DMSO. Under light irradiation, the incubation of 100 μM VB_2 with 100 mM spin-trapping agent DMPO resulted in the formation of the radical adducts.

DMPO was also used as a spin-trapping agent for the detection of $HO^{\bullet}$ (Reaction 3).[37] Solutions were prepared in ultrapure water.

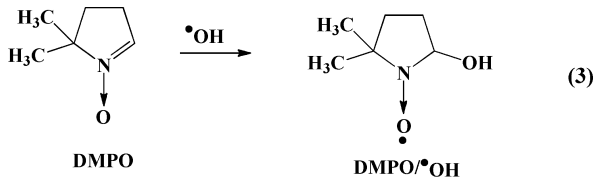

Under light irradiation, the incubation of VB_2 (100 μM) and $FeSO_4$ (10 μM) with 100 mM spin-trapping agent DMPO resulted in the formation of the radical adducts. Then, 200 μL of the freshly prepared mixture was added to a quartz EPR tube and illuminated for 0, 1.0, 2.0 and 3.0 min before recording the EPR spectra.

EPR ROS-Quenching Experiments. To elucidate the mechanism of VB_2-initiated $^{\bullet}OH$ generation, EPR quenching experiments were conducted to examine the effects of the $^1O_2$ quencher (DABCO),[44,45] the $O_2^{\bullet-}$ quencher (1,4-BQ)[44,45] and catalase on the $^{\bullet}OH$ generation. EPR analysis was performed in an aqueous solution (pH 3.0) in the presence of 50 μM DABCO, or 50 μM BQ, or catalase (800 U/mL). Ambient temperature (20 °C) EPR spectra were recorded in an aqueous solution (pH 3.0) at two different irradiation times: 0 min (background) and 1.0 min. Catalase quenching experiments were conducted to assess whether H_2O_2 was the immediate precursor to $^{\bullet}OH$. EPR experiments were also conducted to examine the $^{\bullet}OH$ generation in the presence of a triplet state quencher, CuCN (50 μM) under similar conditions.

NB Photodegradation Experiments. To confirm further the $^{\bullet}OH$ generation, a widely used model reaction, the hydroxylation of nitrobenzene, was employed to evaluate the $^{\bullet}OH$ reactivity.[40,41] Light-mediated hydroxylation of nitrobenzene (25 μM, pH 3.0) was completed via photosensitization of VB_2 (25 μM) in the presence of ferrous ion ($FeSO_4$, 10 μM). Samples were irradiated using a 500 W Xe-arc lamp equipped with an UV-cutoff (>400 nm). The suspension was sequentially photolyzed (20 min), stored in the dark (30 min), and photolyzed (20 min), and aliquots were removed and analyzed at given time intervals. The light dependence of hydroxylation process was monitored using high performance liquid chromatography (HPLC) and the hydroxylation products were validated using gas chromatography/mass spectrometry (GC/MS).

HPLC and GC/MS Analyses. The nitrobenzene hydroxylation process was monitored through measuring the initial and residual nitrobenzene concentrations by an HPLC (1100, Agilent Inc., USA) equipped with a VWD detector and a Hypersil ODS column. A mixture of methanol and water (65:35, v/v) was used as the isocratic mobile phase with 0.1% acetic acid in water. The flow rate was set at

DOI: 10.1021/acssuschemeng.5b00267
ACS Sustainable Chem. Eng. 2015, 3, 1756−1763

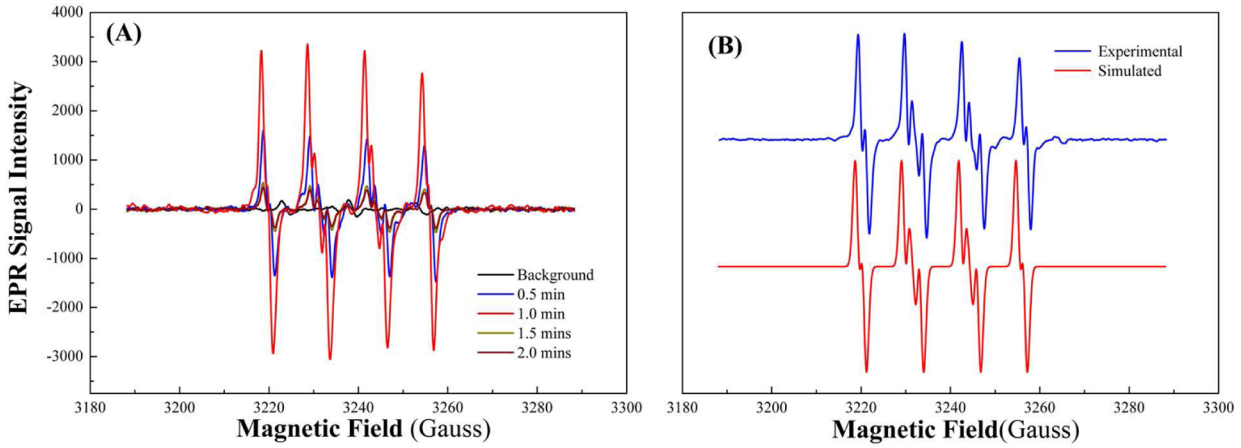

Figure 2. (A) Ambient temperature (20 °C) EPR spectra of DMPO/$O_2^{\bullet-}$ produced by photosensitization of VB_2 under visible irradiation (pH 7.0); (B) simulation of EPR spectra of DMPO/$O_2^{\bullet-}$. Dimethyl sulfoxide was used as a solvent. The solution contained 100 μM VB_2 and 100 mM DMPO. Samples were irradiated with a 500 W Xe-arc lamp equipped with an UV-cutoff (>400 nm). The hyperfine splitting constants for DMPO/$O_2^{\bullet-}$ were a_N = 12.80 G, a_H^{β} = 10.40 G, a_H^{γ} = 1.35 G; g = 2.0021.

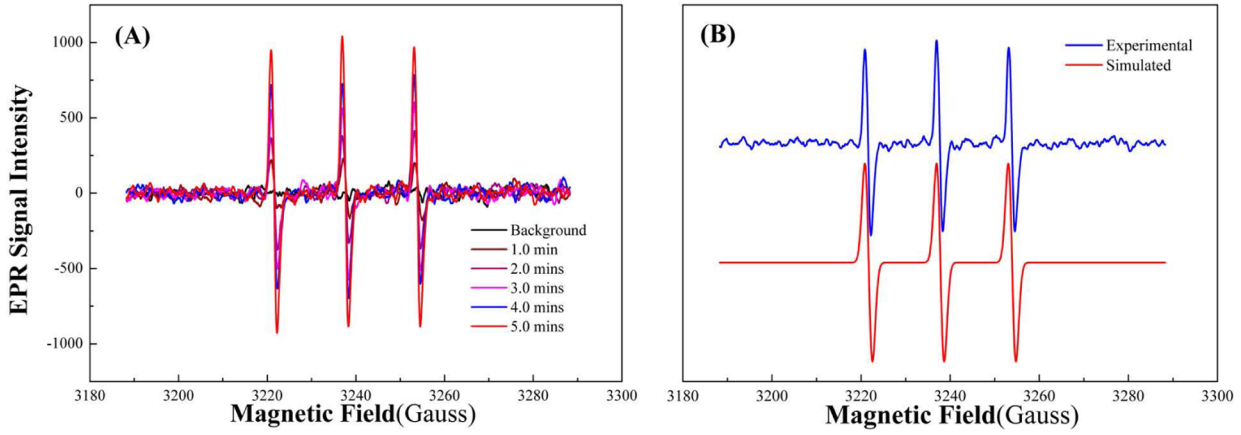

Figure 3. (A) Ambient temperature (20 °C) EPR spectra of 4-oxo-TEMP/$^1O_2$ generated in aqueous solution (pH 7.0) under visible irradiation; (B) simulation of EPR spectra of 4-oxo-TEMP/$^1O_2$. The aqueous solution contained 100 μM VB_2 and 100 mM 4-oxo-TEMP. Samples were irradiated with a 500 W Xe-arc lamp equipped with an UV-cutoff (>400 nm). The hyperfine splitting constants for 4-oxo-TEMP/$^1O_2$ (4-oxo-TEMPO) were a_N = 16.2 G and g = 2.0055.

1.0 mL·min^{-1}, the UV detector was set at 254 nm, and the column temperature was set at 30 °C.

GC/MS was used to analyze the hydroxylation products of nitrobenzene with a Trace GC/DSQ single quadrupole mass spectrometer (Thermo Inc., USA). Before analysis, the irradiated sample solutions were extracted with 10 mL redistilled CH_2Cl_2. The resulting organic phases were decanted, and were then dehydrated by $MgSO_4$ for GC/MS analysis. The GC has a TR-35MS capillary column (30 m × 0.25 mm × 0.25 μm). Helium (99.99%) was used as the carrier gas with a constant flow rate of 1.0 mL/min. An autosampler was used, and split injection was performed at a split ratio of 50. The oven temperature was programmed from 50 °C for 4 min, then at a ramp of 15 °C min^{-1} to 280 °C and held at 280 °C for 3 min. MS was operated under the following conditions: transfer line, 220 °C; ion source, 220 °C; electron energy, 70 eV.

RESULTS AND DISCUSSION

ROS-Generation Photosensitized by VB_2. VB_2 has been reported to act as an excellent photosensitizer to generate reactive oxygen species (ROS), such as singlet oxygen ($^1O_2$) and/or superoxide radical ($O_2^{\bullet-}$). $O_2^{\bullet-}$ is usually recognized as a precursor of most other ROS.[46] Thus, the formation of $O_2^{\bullet-}$ was first confirmed using EPR spectroscopy combined with spin trapping. The hyperfine splitting constants for DMPO/$O_2^{\bullet-}$ were a_N = 12.80 G; a_H^{β} = 10.40 G; a_H^{γ} = 1.35 G; g = 2.0021 (Figure 2A). An accurate EPR spectrum simulation of DMPO/$O_2^{\bullet-}$ has also been performed (Figure 2B).

The specific signals of 4-oxo-TEMP/$^1O_2$ were produced by $^1O_2$ generated from photoexcited VB_2 (Figure 3A).[29,30,33,35] The spectrum is composed of a triplet of lines, with a peak height ratio of 1:1:1, with parameters including hyperfine constants, a_N = 16.2 G and a g-value = 2.0055.[33,35] These parameters exactly matched with accurate EPR spectrum simulation of 4-oxo-TEMP/$^1O_2$ (Figure 3B). The results show the increase of $^1O_2$ production in response to the irradiation time from 0 to 5 min.

On the basis of the formation of both $O_2^{\bullet-}$ and $^1O_2$, we examined the feasibility of VB_2 photosensitization for $^{\bullet}$OH generation in the presence of dissolved iron. Solution of VB_2 (100 μM) and $FeSO_4$ (10 μM) with DMPO (100 mM) was prepared in acidic water (pH 3.0). Then, 200 μL of this freshly prepared mixture was added to a quartz EPR tube and illuminated for 0, 1.0, 2.0 and 3.0 min before recording the EPR spectra. Upon exposure to visible irradiation, a major radical/DMPO adduct was formed and assigned to DMPO/$^{\bullet}$OH

DOI: 10.1021/acssuschemeng.5b00267
ACS Sustainable Chem. Eng. 2015, 3, 1756−1763

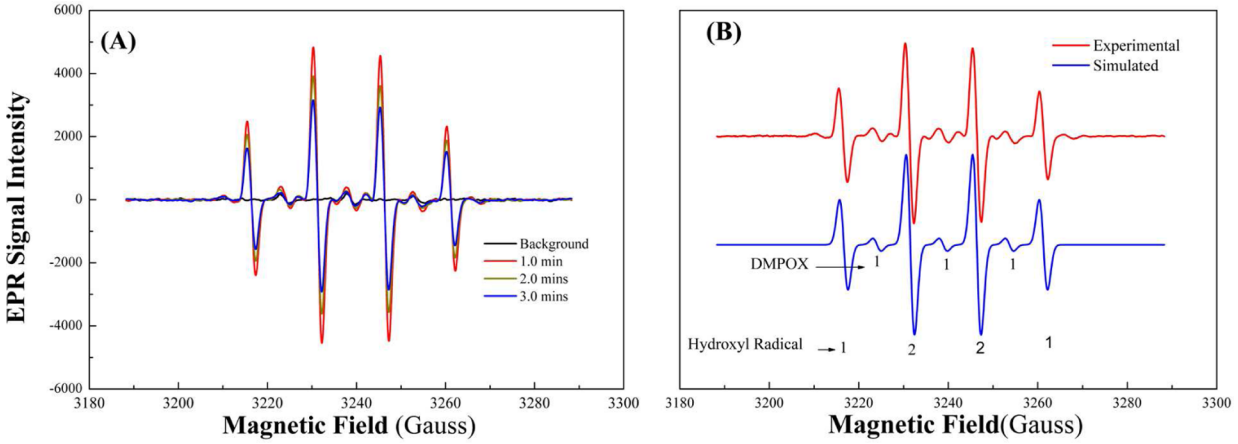

Figure 4. (A) Ambient temperature (20 °C) EPR spectra of DMPO/•OH generated in acidic aqueous solution (pH 3.0) under visible irradiation; (B) simulation of EPR spectra of DMPO/•OH. The aqueous solution contained 100 μM VB_2, 10 μM $FeSO_4$ and 100 mM DMPO. Samples were irradiated with a 500 W Xe-arc lamp equipped with an UV-cutoff (>400 nm). The hyperfine splitting constants for DMPO/•OH were $a_H = a_N$ = 14.96 G and g = 2.0040.

(Figure 4A). The hyperfine splitting constants for DMPO/•OH were $a_H = a_N$ = 14.96 G and a g-value = 2.0040 (Figure 4B).[47,48] Among the signals for DMPO/•OH (1:2:2:1), a weak EPR signal was composed of a triplet of lines with a peak height ratio of 1:1:1. There is a signal of oxidized DMPO (DMPOX) in the EPR spectra. We take this signal of DMPOX into account. A possible mechanism has proposed as follows (Reaction 4):

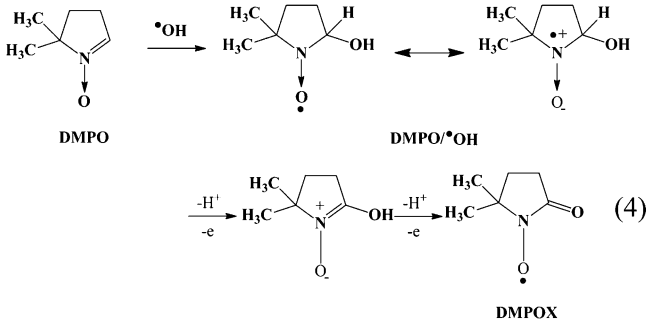

The effect of pH value on the •OH generation was also investigated. The EPR spectra of DMPO/•OH adduct were collected, and the EPR signal intensity ratio at different pH values was $S_{pH3.0}$:$S_{pH7.0}$:$S_{pH11.0}$ = 100:13:2 (Figure 5A). At pH 11.0, the •OH generation was severely inhibited and no obvious signals for DMPO/•OH adduct were detected. Under acidic and/or neutral conditions, ferric ion was also found to benefit for the VB_2-initiated •OH generation process (Figure 5B). Thus, a low pH was favorable for •OH generation, and both ferrous ion and ferric ion were proven to enhance such a process.

Hydroxylation of NB. NB is a typical biorefractory organic pollutant widely present in natural waters. To further confirm the VB_2-initiated •OH generation, we employed the hydroxylation of NB as a model reaction to study •OH reactivity.[38,39] The variation of NB concentration over irradiation time was monitored using high performance liquid chromatography (HPLC) (Figure S1, Supporting Information). A significant decrease in NB level was observed during the photolysis period, demonstrating that hydroxylation was occurring, and this trend

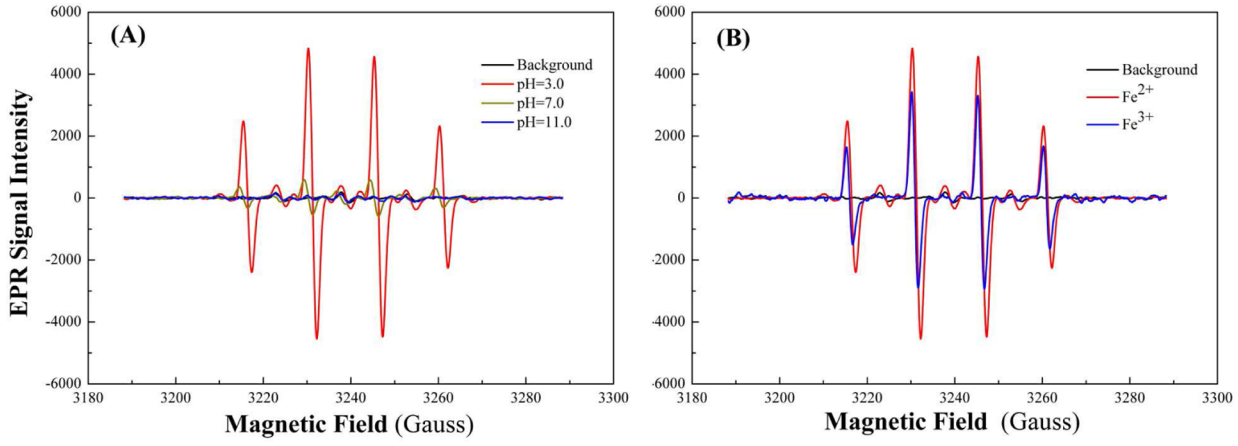

Figure 5. (A) EPR spectra of DMPO/•OH produced by VB_2/Fe^{2+} solution under visible irradiation (1.0 min) with different pH values (3.0, 7.0 and 11.0). The aqueous solution contained 100 μM VB_2, 10 μM $FeSO_4$, and 100 mM DMPO; (B) ambient temperature (20 °C) EPR spectra of DMPO/•OH produced by VB_2 solution (pH 3.0) under 1.0 min visible irradiation in the presence of Fe^{2+} or Fe^{3+}. Solutions contained 100 μM VB_2, 10 μM $FeSO_4$ (or 10 μM $FeCl_3$) and 100 mM DMPO. The pH was adjusted using HCl (1.0 M) or NaOH (1.0 M) solutions. Samples were irradiated using a 500 W Xe-arc lamp equipped with an UV-cutoff (>400 nm).

DOI: 10.1021/acssuschemeng.5b00267
ACS Sustainable Chem. Eng. 2015, 3, 1756−1763

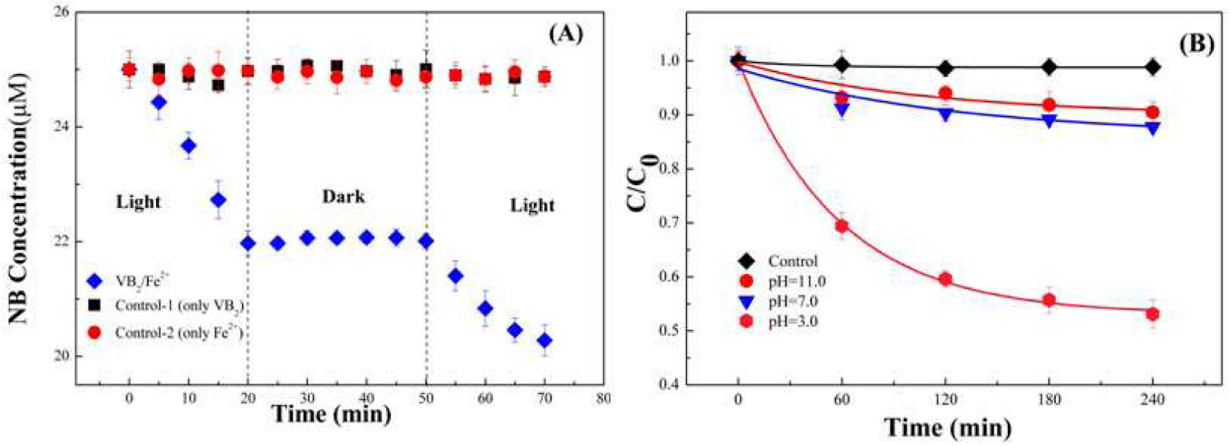

Figure 6. (A) Light-mediated hydroxylation of nitrobenzene (NB) via photosensitization of VB_2 in the presence of ferrous ion. The aqueous solution (pH 3.0) contained 25 μM NB, 25 μM VB_2 and 10 μM $FeSO_4$; NB solution (25 μM, pH 3.0) in the presence of VB_2 (25 μM) without Fe^{2+} was used as Control-1 and NB solution (25 μM, pH 3.0) in the presence of Fe^{2+} (10 μM) without VB_2 was used as Control-2; (B) effect of pH on the NB photodegradation under visible irradiation. NB solution (25 μM) in the presence of VB_2 (25 μM) without Fe^{2+} was used as Control. Samples were irradiated using a 500 W Xe-arc lamp equipped with an UV-cutoff (>400 nm).

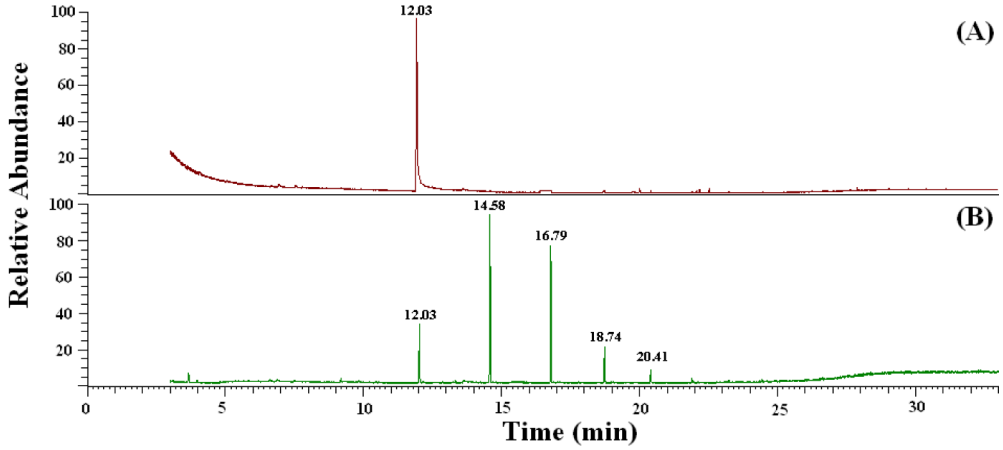

Figure 7. GC/MS analysis of the hydroxylation products of NB. (A) GC chromatogram of initial NB solution, MS spectrum at 12.03 min: m/z = 123.05; (B) GC chromatogram of the hydroxylation result after 1.0 h of visible irradiation. MS spectra at 14.58, 16.79 and 18.74 min: m/z = 139.06, ortho, meta and para products; the hydroxylation products of NB. Initial reaction solution contained 25 μM VB_2, 10 μM $FeSO_4$ and 100 μM nitrobenzene at pH 3.0. Reaction was carried out at ambient temperature (20 °C) in Pyrex-glass reactors irradiated with a 500 W Xe-arc lamp equipped with an UV-cutoff (>400 nm).

terminated immediately in the absence of light (Figure 6A). The results of the control test show that VB_2 and dissolved iron were both required. The photodegradation activities of NB solution were also evaluated under different pHs (pH 3.0, 7.0, 11.0), as shown in Figure 6B. A low pH was favorable for the hydroxylation process, which is in accordance with the EPR results. The hydroxylation products were further validated using gas chromatography/mass spectrometry (GC/MS). The results confirm that NB was attacked by $HO^{\bullet}$ to generate ortho, meta and para products (Figure 7).

Effect of ROS-Quenchers on the $^{\bullet}$OH Generation. To reveal the $^{\bullet}$OH generation process, EPR experiments were conducted to examine the $^{\bullet}$OH generation in the presence of different ROS quenchers. The effect of the $^1O_2$ quencher (1,4-diazabicyclo[2.2.2]octane, DABCO, 50 μM)[40,41] on the $^{\bullet}$OH generation in an aqueous solution (pH 3.0) was first assessed. As shown in Figure 8A, $^1O_2$ quencher (DABCO) had no obvious inhibitory effect against the $^{\bullet}$OH generation. Thus, the participation of $^1O_2$ in the $^{\bullet}$OH generation process could be ruled out. The effect of the $O_2^{\bullet-}$ quencher (1,4-benzoquinone, 1,4-BQ, 50 μM)[41,42] was tested under similar conditions. The EPR results clearly show that the VB_2-initiated $^{\bullet}$OH generation was substantially inhibited through quenching $O_2^{\bullet-}$ by 1,4-BQ (Figure 8B). These results indicate that $O_2^{\bullet-}$ was an important intermediate to produce $^{\bullet}$OH, while $^1O_2$ was not involved in the VB_2-initiated $^{\bullet}$OH generation process.

The lifetime of $O_2^{\bullet-}$ is very short in proton solvents.[35,36] It is sensitive in the presence of proton and is converted to hydrogen peroxide (H_2O_2) quickly in aqueous solution. It is widely presumed that the most abundant $^{\bullet}$OH generation *in vivo* is the transition-metal-ion catalyzed Fenton decomposition of H_2O_2.[37,43] Thus, catalase quenching experiments were conducted to assess whether H_2O_2 was the immediate precursor to $^{\bullet}$OH. EPR spectra were recorded in both acidic aqueous solution (pH 3.0) and neutral aqueous solution (pH 7.0). EPR spectrum of DMPO/$^{\bullet}$OH generated under similar conditions without added catalase was used as the control. The signal intensity of DMPO/$^{\bullet}$OH decreased substantially in the presence of catalase (Figure 8C). A similar experiment result was obtained in neutral aqueous solution (pH 7.0) (Figure S2,

DOI: 10.1021/acssuschemeng.5b00267
ACS Sustainable Chem. Eng. 2015, 3, 1756−1763

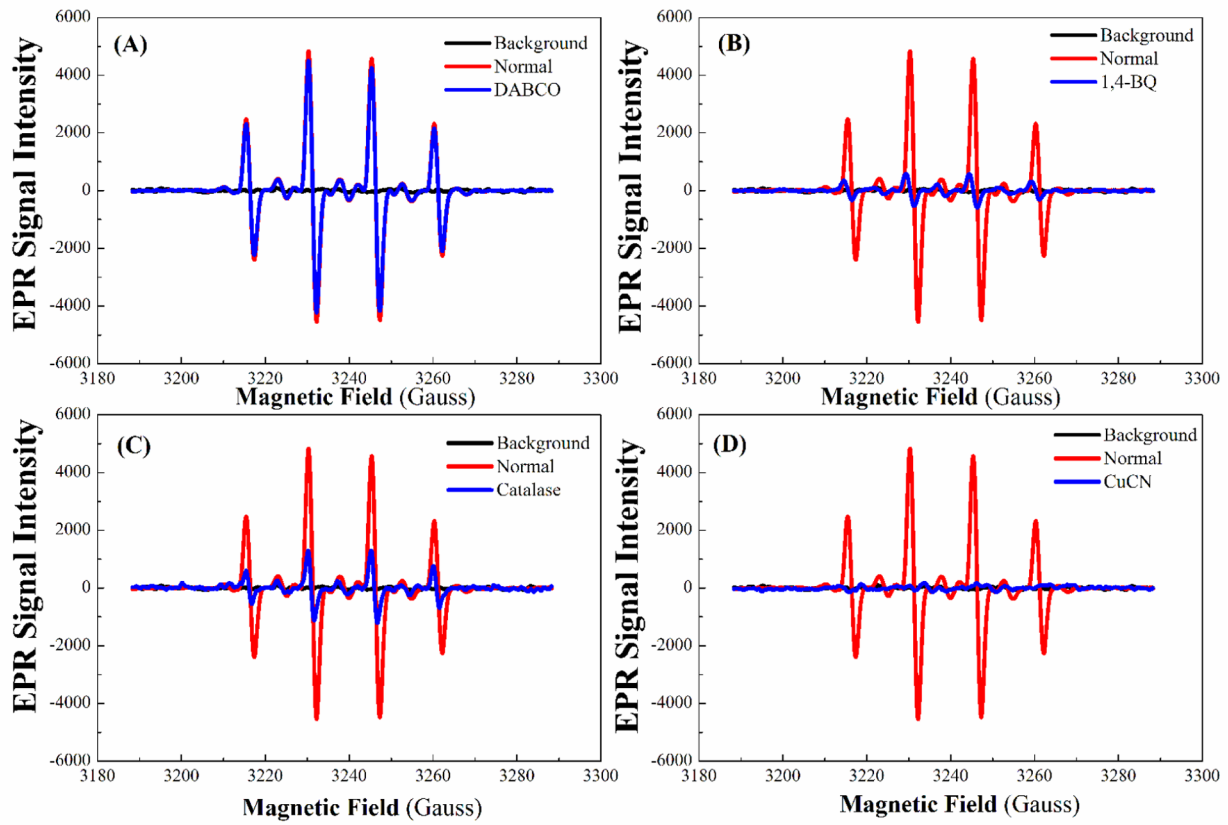

Figure 8. •OH generation in VB_2/Fe^{2+} solution under visible irradiation in the presence of different quenchers: (A) DABCO ($^1O_2$ quencher); (B) 1−4-BQ ($O_2^{\bullet-}$ quencher); (C) catalase (H_2O_2 quencher); (D) CuCN (triplet state quencher).

Supporting Information). EPR experiments were also conducted to examine the •OH generation in the presence of a triplet state quencher, copper cyanide (CuCN). As shown in Figure 8D, the VB_2-initiated •OH generation was inhibited completely in the presence of CuCN, because the triplet state of VB_2 was quenched by CuCN. These results clearly indicate that H_2O_2 and the triplet state of VB_2 were also important intermediates in the VB_2-initiated •OH generation process.

With the analysis above, $^1O_2$ can be excluded from the pathway of VB_2-initiated •OH generation. Thus, a possible mechanism is proposed for the VB_2-initiated •OH generation, as shown in Figure 1. VB_2 plays a dual role of photosensitizer and electron mediator. In the initial step, VB_2 works as an excellent photosensitizer. Upon absorption of a photon, VB_2 gives rise to its excited singlet state ($^1VB^*$) and, through intersystem crossing, to its excited triplet state ($^3VB^*$).[29−31] In the subsequent step, VB_2 works as an effective electron mediator to mediate $O_2^{\bullet-}$ generation. However, $O_2^{\bullet-}$ is sensitive to proton and is converted to H_2O_2 quickly in water. Ultimately, the •OH generation occurs through dissolved-iron catalyzed decomposition of H_2O_2.[37]

In summary, an efficient method for •OH generation is developed in this study. The significance of this study lies in the elucidation of the VB_2-initiated •OH generation process, which is useful to providing interesting insights into the degradation of environmental contaminants and the biogeochemical cycling of elements in natural aquatic ecosystems. In addition, all ingredients involved in this process are nontoxic, environmentally benign and easily available. Thus, this process might have some potential environmental implications, and even might be used to strengthen the remove efficiency of biorefractory pollutants in water and wastewater treatment systems. However, the VB_2-initiated •OH generation is a very complex process. There are some differences in the conditions used in this laboratory experiment and those of practical applications. Thus, further in-depth investigations are warranted.

■ ASSOCIATED CONTENT

Supporting Information

HPLC chromatograms (absorption at 254 nm) of the NB/VB_2/Fe^{2+} solutions at different irradiation times (Figure S1) and effects of catalase on the •OH generation produced by VB_2/Fe^{2+} solution under neutral conditions (Figure S2). The Supporting Information is available free of charge on the ACS Publications website at DOI: 10.1021/acssuschemeng.5b00267.

■ AUTHOR INFORMATION

Corresponding Author

*Han-Qing Yu. Fax: +86 551 63601592. E-mail: hqyu@ustc.edu.cn.

Notes

The authors declare no competing financial interest.

■ ACKNOWLEDGMENTS

The authors thank the National Basic Research Program of China (2011CB933702), the National Science Foundation of China (21207031) and the Program for Changjiang Scholars

DOI: 10.1021/acssuschemeng.5b00267
ACS Sustainable Chem. Eng. 2015, 3, 1756−1763

and Innovative Research Team in University, China for the partial support of this study.

REFERENCES

(1) Matson, P. A.; Parton, W. J.; Power, A. G.; Swift, M. J. Agricultural intensification and ecosystem properties. *Science* **1997**, *277*, 504−509.
(2) Ter Halle, A.; Richard, C. Simulated solar light irradiation of mesotrione in natural waters. *Environ. Sci. Technol.* **2008**, *42*, 301−307.
(3) Menager, M.; Sarakha, M. Simulated solar light photo-transformation of organophosphorus azinphos methyl at the surface of clays and goethite. *Environ. Sci. Technol.* **2013**, *47*, 765−772.
(4) Xu, H. M.; Cooper, W. J.; Jung, J.; Song, W. H. Photosensitized degradation of amoxicillin in natural organic matter isolate solutions. *Water Res.* **2011**, *45*, 632−638.
(5) Watkinson, A. J.; Murby, E. J.; Costanzo, S. D. Removal of antibiotics in conventional and advanced wastewater treatment: Implications for environmental discharge and wastewater recycling. *Water Res.* **2007**, *41*, 4164−4176.
(6) Scherson, Y. D.; Criddle, C. S. Recovery of freshwater from wastewater: Upgrading process configurations to maximize energy recovery and minimize residuals. *Environ. Sci. Technol.* **2014**, *48*, 8420−8432.
(7) Díaz-Cruz, M. S.; Barceloí, D. Trace organic chemicals contamination in ground water recharge. *Chemosphere* **2008**, *72*, 333−342.
(8) Wintgens, T.; Salehi, F.; Hochstrat, R.; Melin, T. Emerging contaminants and treatment options in water recycling for indirect potable use. *Water Sci. Technol.* **2008**, *57*, 99−107.
(9) Xu, G. H.; Chance, M. R. Hydroxyl radical-mediated modification of proteins as probes for structural proteomics. *Chem. Rev.* **2007**, *107*, 3514−3543.
(10) Zepp, R. G.; Hoigne, J.; Bader, H. Nitrate-induced photo-oxidation of trace organic chemicals in water. *Environ. Sci. Technol.* **1987**, *21*, 443−450.
(11) Brekken, J. F.; Brezonik, P. L. Indirect photolysis of acetochlor: Rate constant of a nitrate-mediated hydroxyl radical reaction. *Chemosphere* **1998**, *36*, 2699−2704.
(12) Pérez-Estrada, L. A.; Malato, S.; Gernjak, W.; Agüera, A.; Thurman, E. M.; Ferrer, I.; Fernández-Alba, A. R. Photo-Fenton degradation of diclofenac: Identification of main intermediates and degradation pathway. *Environ. Sci. Technol.* **2005**, *39*, 8300−8306.
(13) Sirtori, C.; Zapata, A.; Oller, I.; Gernjak, W.; Agüera, A.; Malato, S. Solar photo-Fenton as finishing step for biological treatment of a pharmaceutical wastewater. *Environ. Sci. Technol.* **2009**, *43*, 1185−1191.
(14) Zepp, R. G.; Wolfe, N. L.; Baughman, G. L.; Hollis, R. C. Singlet oxygen in natural-waters. *Nature* **1977**, *267*, 421−423.
(15) Zhang, T.; Hsu-Kim, H. Photolytic degradation of methylmercury enhanced by binding to natural organic ligands. *Nat. Geosci.* **2010**, *3*, 473−476.
(16) Cory, R. M.; McNeill, K.; Cotner, J. P.; Amado, A.; Purcell, J. M.; Marshall, A. G. Singlet oxygen in the coupled photochemical and biochemical oxidation of dissolved organic matter. *Environ. Sci. Technol.* **2010**, *44*, 3683−3689.
(17) Latch, D. E.; McNeill, K. Microheterogeneity of singlet oxygen distributions in irradiated humic acid solutions. *Science* **2006**, *311*, 1743−1747.
(18) Fujii, M.; Rose, A. L.; Waite, T. D.; Omura, T. Oxygen and superoxide-mediated redox kinetics of iron complexed by humic substances in coastal seawater. *Environ. Sci. Technol.* **2010**, *44*, 9337−9342.
(19) Avetta, P.; Bella, F.; Bianco Prevot, A.; Laurenti, E.; Montoneri, E.; Arques, A.; Carlos, L. Waste cleaning waste: Photodegradation of monochlorophenols in the presence of waste-derived photosensitizer. *ACS Sustainable Chem. Eng.* **2013**, *1*, 1545−1550.
(20) Brezonik, P. L.; Fulkerson-Brekken, J. Nitrate-induced photolysis in natural waters: Controls on concentrations of hydroxyl radical photo-intermediates by natural scavenging agents. *Environ. Sci. Technol.* **1998**, *32*, 3004−3010.
(21) Southworth, B. A.; Voelker, B. M. Hydroxyl radical production via the photo-Fenton reaction in the presence of fulvic acid. *Environ. Sci. Technol.* **2003**, *37*, 1130−1136.
(22) Dong, M. M.; Rosario-Ortiz, F. L. Photochemical formation of hydroxyl radical from effluent organic matter. *Environ. Sci. Technol.* **2012**, *46*, 3788−3794.
(23) Song, W. H.; Yan, S. W.; Cooper, W. J.; Dionysiou, D. D.; O'Shea, K. E. Hydroxyl radical oxidation of cylindrospermopsin (cyanobacterial toxin) and its role in the photochemical transformation. *Environ. Sci. Technol.* **2012**, *46*, 12608−12615.
(24) Buschmann, J.; Canonica, S.; Sigg, L. Photoinduced oxidation of antimony(III) in the presence of humic acid. *Environ. Sci. Technol.* **2005**, *39*, 5335−5341.
(25) Voelker, B. M.; Morel, F. M. M.; Sulzberger, B. Iron redox cycling in surface waters: Effects of humic substances and light. *Environ. Sci. Technol.* **1997**, *31*, 1004−1011.
(26) Canstein, H.; Ogawa, J.; Shimizu, S.; Lloyd, J. R. Secretion of flavins by *Shewanella* species and their role in extracellular electron transfer. *Appl. Environ. Microbiol.* **2008**, *7*, 615−623.
(27) Marsili, E.; Baron, D. B.; Shikhare, I. D.; Coursolle, D.; Gralnick, J. A.; Bond, D. R. *Shewanella* secretes flavins that mediate extracellular electron transfer. *Proc. Natl. Acad. Sci. U. S. A.* **2008**, *105*, 3968−3973.
(28) Sanudo-Wilhelmy, S. A.; Cutter, L. S.; Durazo, R.; Smail, E. A.; Gomez-Consarnau, L.; Webb, E. A.; Prokopenko, M. G.; Berelson, W. M.; D. M. Karl, D. M. Multiple B-vitamin depletion in large areas of the coastal ocean. *Proc. Natl. Acad. Sci. U. S. A.* **2012**, *109*, 14041−14045.
(29) Haggi, E.; Bertolotti, S.; Garcia, N. A. Modelling the environmental degradation of water contaminants. Kinetics and mechanism of the riboflavin-sensitised-photooxidation of phenolic compounds. *Chemosphere* **2004**, *55*, 1501−1507.
(30) Remucal, C. K.; McNeill, K. Photosensitized amino acid degradation in the presence of riboflavin and its derivatives. *Environ. Sci. Technol.* **2011**, *45*, 5230−5237.
(31) Xu, F.; Song, X. N.; Sheng, G. P.; Luo, H. W.; Li, W. W.; Yao, R. S.; Yu, H. Q. Sunlight-mediated degradation of methyl orange sensitized by riboflavin: Roles of reactive oxygen species. *Sep. Purif. Technol.* **2015**, *142*, 18−24.
(32) Ishikawa, K.; Takenaga, K.; Akimoto, M.; Koshikawa, N.; Yamaguchi, A.; Imanishi, H.; Nakada, K.; Honma, Y.; Hayashi, J. ROS-generating mitochondrial DNA mutations can regulate tumor cell metastasis. *Science* **2008**, *320*, 661−664.
(33) Moan, J.; Wold, E. Detection of singlet oxygen production by ESR. *Nature* **1979**, *279*, 450−451.
(34) Kumar, S. S.; Devasagayam, T. P. A.; Bhushan, B.; Verma, N. C. Scavenging of reactive oxygen species by chlorophyllin: An ESR study. *Free Radical Res.* **2001**, *35*, 563−574.
(35) Yamakoshi, Y.; Umezawa, N.; Ryu, A.; Arakane, K.; Miyata, N.; Goda, Y.; Masumizu, T.; Nagano, T. Active oxygen species generated from photoexcited fullerene (C_{60}) as potential medicines: $O_2^{\bullet-}$ versus $^1O_2$. *J. Am. Chem. Soc.* **2003**, *125*, 12803−12809.
(36) Pieta, P.; Petr, A.; Kutner, W.; Dunsch, L. In situ ESR spectroscopic evidence of the spin-trapped superoxide radical, $O_2^{\bullet-}$, electrochemically generated in DMSO at room temperature. *Electrochim. Acta* **2008**, *53*, 3412−3415.
(37) Burkitt, M. J.; Mason, R. P. Direct evidence for in vivo hydroxyl-radical generation in experimental iron overload: An ESR spin-trapping investigation. *Proc. Natl. Acad. Sci. U. S. A.* **1991**, *88*, 8440−8444.
(38) Roberts, J. L.; Morrison, M. M.; Sawyer, D. T. Base-induced generation of superoxide ion and hydroxyl radical from hydrogen peroxide. *J. Am. Chem. Soc.* **1978**, *100*, 329−330.
(39) Luo, W. C.; Muller, J. G.; Burrows, C. J. The pH-dependent role of superoxide in riboflavin-catalyzed photooxidation of 8-oxo-7,8-dihydroguanosine. *Org. Lett.* **2001**, *3*, 2801−2804.

DOI: 10.1021/acssuschemeng.5b00267
ACS Sustainable Chem. Eng. 2015, 3, 1756−1763

(40) Feng, J.; Aki, S. N. V. K.; Chateauneuf, J. E.; Brennecke, J. F. Hydroxyl radical reactivity with nitrobenzene in subcritical and supercritical water. *J. Am. Chem. Soc.* **2002**, *124*, 6304−6311.
(41) Zhang, S. J.; Jiang, H.; Li, M. J.; Yu, H. Q.; Yin, H.; Li, Q. R. Kinetics and mechanisms of radiolytic degradation of nitrobenzene in aqueous solutions. *Environ. Sci. Technol.* **2007**, *41*, 1977−1982.
(42) Barbieri, Y.; Massad, W. A.; Diaz, D. J.; Sanz, J.; Amat-Guerri, F.; Garcia, N. A. Photodegradation of bisphenol A and related compounds under natural-like conditions in the presence of riboflavin: Kinetics, mechanism and photoproducts. *Chemosphere* **2008**, *73*, 564−571.
(43) Hanamura, M.; Kamada, J.; Amano, A.; Takeuchi, K.; Okazaki, T.; Hirai, K.; Kitagawa, T. Self-sensitized photooxygenation of a C_{60}−cycloheptatriene dyad to form norcaradiene-derived endoperoxides. *Eur. J. Org. Chem.* **2010**, *17*, 3257−3264.
(44) Stylidi, M.; Kondarides, D. I.; Verykios, X. E. Visible light-induced photocatalytic degradation of Acid Orange 7 in aqueous TiO_2 suspensions. *Appl. Catal., B* **2004**, *47*, 189−201.
(45) Zhao, S.; Wang, X. H.; Huo, M. X. Catalytic wet air oxidation of phenol with air and micellar molybdovanadophosphoric polyoxometalates under room condition. *Appl. Catal., B* **2010**, *97*, 127−134.
(46) Balaban, R. S.; Nemoto, S.; Finkel, T. Mitochondria, oxidants, and aging. *Cell* **2005**, *120*, 483−495.
(47) Sugiyama, M. Effects of vitamins on chromium(VI)-induced damage. *Environ. Health Perspect.* **1991**, *92*, 63−70.
(48) Sel, S.; Nass, N.; Pötzsch, S.; Trau, S.; Simm, A.; Kalinski, T.; Duncker, G. I-W.; Kruse, F. E.; Auffarth, G. U.; Brömme, H.-J. UVA irradiation of riboflavin generates oxygen-dependent hydroxyl radicals. *Redox Rep.* **2014**, *19*, 72−79.

DOI: 10.1021/acssuschemeng.5b00267
ACS Sustainable Chem. Eng. 2015, 3, 1756−1763